Analysis of the RNA-Editing Reaction of ADAR2 with Structural and Fluorescent Analogues of the GluR-B R/G Editing Site†

Olen M. Stephens,‡ Hye Young Yi-Brunozzi,‡ and Peter A. Beal*

Department of Chemistry, University of Utah, Salt Lake City, Utah 84112

Received May 22, 2000; Revised Manuscript Received July 17, 2000

ABSTRACT: ADARs are adenosine deaminases responsible for RNA editing reactions that occur in eukaryotic pre-mRNAs, including the pre-mRNAs of glutamate and serotonin receptors. Here we describe the generation and analysis of synthetic ADAR2 substrates that differ in structure around an RNA editing site. We find that five base pairs of duplex secondary structure 5′ to the editing site increase the single turnover rate constant for deamination 17−39-fold when compared to substrates lacking this structure. ADAR2 deaminates an adenosine in the sequence context of a natural editing site >90-fold more rapidly and to a higher yield than an adjacent adenosine in the same RNA structure. This reactivity is minimally dependent on the base pairing partner of the edited nucleotide; adenosine at the editing site in the naturally occurring A·C mismatch is deaminated to approximately the same extent and only 4 times faster than adenosine in an A·U base pair at this site. A steady-state rate analysis at a saturating concentration of the most rapidly processed substrate indicates that product formation is linear with time through at least three turnovers with a slope of 13 ± 1.5 nM·min^{-1} at 30 nM ADAR2 for a k_{ss} = 0.43 ± 0.05 min^{-1}. In addition, ADAR2 induces a 3.3-fold enhancement in fluorescence intensity and a 14 nm blue shift in the emission maximum of a duplex substrate with 2-aminopurine located at the editing site, consistent with a mechanism whereby ADAR2 flips the reactive nucleotide out of the double helix prior to deamination.

RNA editing is a term used to describe the structural alteration, insertion, or deletion of nucleotides in RNA (*1*). If the modification occurs in messenger RNA (mRNA), it can result in the translation of a protein sequence different from that predicted by the DNA sequence of the gene. A number of mRNA sequences from a variety of organisms are now known to arise from RNA editing (*2*−*4*). Thus, this process can play an essential role in the transfer of genetic information that takes place during protein expression.

Processing of the mRNA for mammalian GluR-B,[1] a subunit of a glutamate-gated ion channel, involves editing reactions where genomically encoded sequences are altered in the pre-mRNA by deamination of adenosine (*4*). The deamination of adenosine (A) in the mRNA results in inosine (I) at that position (Figure 1). Because inosine is translated as guanosine (G), the editing reaction causes a functional G for A replacement. At one of the editing sites in the GluR-B pre-mRNA (the R/G site), an arginine codon is converted to a sequence that encodes glycine (*5*). Receptors containing B subunits with glycine at this position have been shown to recover from desensitization at different rates than those with arginine at this position (*5*). Specific deamination sites in other pre-mRNA sequences have also been identified (*3*).

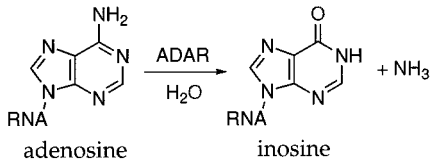

FIGURE 1: RNA editing adenosine deamination reaction catalyzed by ADARs.

ADAR2 is an approximately 80 kDa protein that efficiently deaminates the R/G site of GluR-B pre-mRNA sequences in vitro (*6*, *7*). This enzyme has two copies of a protein sequence (dsRBM) found in double-stranded-RNA binding proteins such as PKR, the RNA-dependent protein kinase, and staufen, a *Drosophila* RNA transport protein (*8*). Consistent with the presence of dsRBMs in ADAR2, duplex RNA secondary structure in the substrate is a requirement for the ADAR2-catalyzed reaction.

C-terminal to the RNA binding motifs, amino acid sequences have been identified that may comprise the deamination active site (*9*, *10*). Nucleoside deaminases, such as adenosine deaminase (ADA) and cytidine deaminase (CDA), have been extensively characterized structurally and mechanistically (*11*). ADA and CDA are metalloenzymes that use a zinc-activated water molecule to carry out

† This work was supported by a grant from the Petroleum Research Fund to P.A.B. (ACS-PRF# 32085-G4).

* To whom correspondence should be addressed. Tel: 801-585-9719, FAX: 801-581-8433, E-mail: beal@chemistry.chem.utah.edu.

‡ The first two authors contributed equally to this work.

[1] Abbreviations: ADAR, adenosine deaminase that acts on RNA; bp, base pair(s); nt, nucleotide(s); dsRBM, double-stranded RNA binding motif; THF, tetrahydrofuran; UV, ultraviolet; SDS, sodium dodecyl sulfate; EDTA, ethylenediaminetetraacetic acid; Tris, tris-(hydroxymethyl)aminomethane; DTT, dithiothreitol; TBE, 90 mM Tris, 90 mM boric acid, 2 mM EDTA; PAGE, polyacrylamide gel electrophoresis; TE, 10 mM TrisHCl, pH 7.5, 0.1 mM EDTA; GluR-B, glutamate receptor B subunit; ADA, adenosine deaminase; CDA, cytidine deaminase; PKR, RNA-dependent protein kinase; R/G site, arginine to glycine editing site in GluR-B pre-mRNA; 2-AP, 2-aminopurine; λ^{ex}, excitation wavelength; M.*Eco*RI, *Eco*RI N6 adenosine methyltransferase; M.*Taq*I, *Taq*I N6 adenosine methyltransferase.

10.1021/bi0011577 CCC: $19.00
Published on Web 09/08/2000

hydrolytic deamination of their nucleoside substrates. The active sites of these enzymes are composed of amino acid sequences that are highly conserved among species. These residues provide the ligands to the active site zinc and the acidic/basic groups for the necessary proton transfers. The ADARs and a related family of yeast tRNA-specific adenosine deaminases have conserved amino acid sequences similar to the consensus sequence that makes up the active site of CDA (*12*). Using the comparison to CDA, amino acids identified as possible active site residues for the ADARs have been altered in ADAR1 by site-directed mutagenesis with a corresponding loss of editing activity (*9*). Earlier, Bass and co-workers reported that the source of the oxygen atom present in the product of the ADAR reaction is water, as is true for the nucleoside deaminases (*13*).

These observations suggest that the deamination steps in the reaction mechanism for the ADARs may be similar to those found for the nucleoside deaminases. One major difference between the nucleoside deaminases and the ADARs is the requirement for duplex RNA structure in the ADAR substrate (*13*). However, the contribution of local RNA structure and sequence to the rate of adenosine deamination is poorly understood. While the necessary trajectory of an attacking water for hydrolytic deamination of adenosine makes it likely that the reactive nucleotide is flipped out of the duplex during the reaction, no experimental evidence has been reported for an ADAR-induced base flipping.

Herein we describe the generation of R/G editing site analogues from GluR-B pre-mRNA that differ in structure around the editing site. These substrates have been studied using deamination kinetics and equilibrium binding, and by monitoring enzyme induced-changes in the fluorescence of 2-aminopurine (2-AP)-labeled RNA. These experiments demonstrate a role in transition state stabilization for duplex RNA flanking the editing site. The deamination rate is highly sensitive to the RNA sequence context of the edited adenosine but relatively insensitive to its base pairing partner. Furthermore, we observe changes in the 2-AP fluorescence induced by ADAR2, which constitutes the first experimental evidence for an RNA conformational change during the ADAR2-catalyzed RNA-editing reaction.

MATERIALS AND METHODS

General. Distilled, deionized water was used for all aqueous reactions and dilutions. Biochemical reagents were obtained from Sigma/Aldrich unless otherwise noted. Common enzymes were purchased from Stratagene, Boehringer-Mannheim, or New England Biolabs. Oligonucleotides were prepared on a Perkin-Elmer/ABI model 392 DNA/RNA synthesizer with β-cyanoethyl phosphoramidites. 5′-Dimethoxytrityl-protected 2′-deoxyadenosine, 2′-deoxyguanosine, 2′-deoxycytidine, and thymidine phosphoramidites were purchased from Perkin-Elmer/ABI. Protected adenosine, guanosine, cytidine, uridine, and 2-aminopurine ribonucleoside phosphoramidites were purchased from Glen Research. [γ-^{32}P]ATP (6000 Ci/mmol) was obtained from DuPont NEN. Storage phosphor autoradiography was carried out using imaging plates obtained from Kodak. A Molecular Dynamics STORM 840 was used to obtain all data from phosphor imaging plates. Liquid scintillation counting was carried out with a Beckman LS 6500 Scintillation Counter and Bio-Safe II cocktail from Research Products International, Corp.

Protein Overexpression and Purification. ADAR2 was overexpressed in *S. cerevisiae* containing the human ADAR2 gene under the transcriptional control of a galactose-inducible GAL1 promoter. This expression system and the purification protocol employed were developed by Herbert L. Ley III and Prof. Brenda Bass, Department of Biochemistry, University of Utah (manuscript in preparation). Fractions from the final purification step containing the protein were combined, and the buffer was exchanged with the storage buffer [50 mM Tris-HCl (pH 7.9), 200 mM KCl, 5 mM EDTA, 10% glycerol, 0.01% NP-40, 1 mM DTT] on a Sephadex G-50 column. The protein was then aliquoted and stored at −80 °C. A standard curve for protein concentration was generated by resolving known amounts of BSA, lysozyme, and IgG on a 10% SDS−PAGE gel, visualizing the bands by SyproOrange (BioRad) staining, and quantifying band intensities with a Molecular Dynamics STORM 840 PhosphorImager and ImageQuant software. The standard curve generated was then used to determine the ADAR2 concentration.

Preparation of Duplex RNAs. Deprotection of synthetic oligoribonucleotides was carried out in NH_3-saturated methanol for 24 h at room temperature followed by 0.1 M tetrabutylammonium fluoride in THF for 48 h at room temperature. Deprotected oligonucleotides were purified by PAGE, visualized by UV shadowing, and extracted from the gel by the crush and soak method with 0.5 M NH_4OAc, 0.1% SDS, 0.1 mM EDTA. The oligonucleotides were ethanol-precipitated and redissolved in deionized water. Concentrations were determined by the UV absorbance at 260 nm using extinction coefficients calculated based on the nearest-neighbor approximation (*14*). For the formation of labeled duplex RNA, a given oligonucleotide was labeled at the 5′ end using [γ-^{32}P]ATP (6000 Ci/mmol) and T4 polynucleotide kinase. The unincorporated [γ-^{32}P]ATP was removed using a Microspin G-25 column (Amersham Pharmacia). To the labeled strand was added a known amount (>70-fold excess) of unlabeled strand of the same sequence. The specific activity of this sample was then determined by liquid scintillation counting. The labeled strand was hybridized to the unlabeled complement in TE buffer (10 mM Tris-HCl, pH 7.5, 0.1 mM EDTA) with 50 mM NaCl. The mixture was heated at 95 °C for 5 min and allowed to slow-cool overnight to room temperature. The duplex was purified on a 16% nondenaturing polyacrylamide gel. The appropriate band was visualized by storage phosphor autoradiography, excised, and extracted into TE buffer overnight at room temperature. Polyacrylamide particles were removed using a Spin-X (Costar) centrifuge column. The RNA duplex was ethanol-precipitated, redissolved in deionized water, and stored at −20 °C. The concentration was determined using scintillation counting and the specific activity of the labeled strand.

Construction of Internally Labeled RNA Substrates. The synthesis of substrates containing nucleotides 5′ to the R/G site was based on splint ligations as outlined by Moore and Sharp (*15*). A 22 nt RNA oligonucleotide (30 pmol) (5′-AGGUGGGUGGAAUAGUAUAACA-3′) was 5′-end-

labeled with [γ-^{32}P]ATP and T4 polynucleotide kinase. The buffer was exchanged using a Microspin G-25. The labeled 22-mer was lyophilized into a thin-walled PCR tube at low heat. The lyophilized pellet was redissolved with 3 μL of a 10 μM solution of DNA splint (5′-CTATTCCACCCACCT-TAATGAGGATCCTTTAGG-3′), 2 μL of 20 μM 18-mer RNA oligonucleotide (5′-CCUAAAGGAUCCUCAUUA-3′), 0.5 μL of RNasin from Promega (1.6 units/μL), and 1 μL of NEB T4 DNA ligase 10× buffer [1× conditions: 50 mM Tris-HCl (pH 7.5), 10 mM $MgCl_2$, 10 mM dithiothreitol, 1 mM ATP, 25 μg/mL bovine serum albumin]. This reconstituted solution was heated to 65 °C and slowly cooled to 22 °C over 30 min using a Perkin-Elmer GeneAmp PCR System 2400. To the solution were added 0.5 μL of RNasin, 0.5 μL of 5.5 mM ATP, and 1.5 μL of T4 DNA ligase (45 Weiss units). The reaction was incubated at 30 °C for 6 h and achieved a ligation efficiency of ~70%. RQ1 RNase-free DNase (2 units) was added. The solution was heated to 37 °C for 10 min, cooled to 22 °C for 2 min, and heat-inactivated at 65 °C for 10 min. The sample was purified to nucleotide resolution by PAGE. The product band was visualized by storage phosphor autoradiography and excised. The labeled and ligated oligonucleotide was extracted from the gel slice. To the labeled strand was added a known amount (>70-fold excess) of unlabeled strand of the same sequence. The specific activity of this sample was then determined by liquid scintillation counting. The strands were hybridized, and the resulting duplex was gel-purified and quantified as described above. For the generation of substrate (**g**) with the adenosine adjacent to the R/G site labeled, the oligonucleotide 5′-AAGGUGGGUGGAAUAGUAUAACA-3′ was 5′-end-labeled and ligated to 5′-CCUAAAGGAUC-CUCAUU-3′ using the same DNA splint described above.

*Splint Ligation for Substrate (**e**).* To eliminate the 13 nt 5′ overhang from substrate (**a**), a chimeric extension strand was constructed for the splint ligation 5′-dCdCdTdAdAd-AdGdGdAdTdCdCdTrCrArUrUrA-3′, where dC, dT, dA, and dG are deoxyribonucleotides and rC, rA, and rU are ribonucleotides. This strand was synthesized on a Perkin-Elmer/ABI model 392 DNA/RNA synthesizer with β-cyanoethyl phosphoramidites, using a normal rA column and RNA protocols for coupling, deprotection, and purification. The splint ligation was performed as described above. Following the DNase treatment, the product was purified to nucleotide resolution by PAGE and visualized by storage phosphor autoradiography. The 27-mer internally labeled product was extracted from the gel. To the labeled strand was added a known amount (>70-fold excess) of unlabeled strand of the same sequence. The specific activity of this sample was then determined by liquid scintillation counting. The strands were hybridized, and the resulting duplex was gel-purified and quantified as described above.

Deamination Assay. Each single turnover reaction was carried out with 100 nM ADAR2, 25 nM labeled RNA duplex, and assay buffer containing 15 mM Tris-HCl, pH 7.1, 3% glycerol, 0.5 mM DTT, 60 mM KCl, 1.5 mM EDTA, 0.003% NP-40, 160 units/mL RNasin, and 1.0 μg/mL yeast $tRNA^{Phe}$. Reaction mixtures were incubated at 30 °C for varying times. At each time point, an aliquot was removed and the reaction was quenched by the addition of 0.5% SDS at 95 °C, followed by digestion with nuclease P1 and resolution of the resulting 5′-mononucleotides by thin-layer chromatography (TLC) as previously described (*16*). Storage phosphor imaging plates (Kodak) were pressed flat against TLC plates and exposed in the dark. The data were analyzed by performing volume integrations of the regions corresponding to starting material, product, and background sites using the ImageQuant software. The data were fit to the equation: $[P]_t = \alpha[1 - e^{(-k_{deam}t)}]$, where $[P]_t$ is the concentration of inosine containing product at time t, α is the fitted reaction end point, and k_{deam} is the fitted rate constant.

For measurement of the steady-state rate of deamination of substrate (**a**), 30 nM ADAR2 was combined with 800 nM labeled RNA substrate in the assay buffer described above. Reaction mixtures were incubated at 30 °C for varying times, and aliquots were removed, quenched, and analyzed by TLC as described above. Product formation was linear with time for the first 7 min, and the reaction rate was obtained from the slope of a linear fit to these data. The reported steady-state rate constant, k_{ss}, was obtained from the equation: rate = k_{ss}[ADAR2].

Gel Mobility Shift Assay. Each binding reaction was carried out by combining ADAR2 at varying concentrations with ~50 pM 5′-^{32}P end-labeled RNA duplex in 15 mM Tris-HCl, pH 7.9, 3% glycerol, 0.5 mM DTT, 60 mM KCl, 1.5 mM EDTA, 0.003% NP-40, 160 units/mL RNasin, and 1.0 μg/mL yeast $tRNA^{Phe}$ and allowing the mixture to incubate at 30 °C for 20 min. Samples were then loaded onto a running 6% nondenaturing polyacrylamide gel (79:1 acrylamide:bisacrylamide) and electrophoresed in 0.5× TBE buffer at 4 °C. Storage phosphor imaging plates (Kodak) were pressed flat against the electrophoresis gels and exposed in the dark. The data were analyzed by performing volume integrations of the regions corresponding to free RNA, the ADAR2·RNA complex, and background sites using the ImageQuant software. For the determination of apparent dissociation constants, the data were fit to the equation: fraction bound = [ADAR2]/([ADAR2] + K_d^{app}) using the least-squares method of KaleidaGraph.

Synthesis and Analysis of Fluorescent RNA Substrates. The 2-aminopurine (2-AP) containing oligoribonucleotide was deprotected with 10 M $MeNH_2$ for 6 h at 35 °C followed by 0.1 M tetrabutylammonium fluoride in THF for 24 h at 35 °C and gel-purified as described above. The extinction coefficient at 260 nm for this oligonucleotide was determined by calculating the sum of the extinction coefficients of the component nucleotides using 1000 $cm^{-1}\cdot M^{-1}$ for 2-AP. Annealing was performed by adding 400 pmol of the 2-AP-containing strand with 600 pmol of the complementary strand in 200 μL of 15 mM Tris-HCl, pH 7.5, 3% glycerol, 60 mM KCl, 1.5 mM EDTA, 0.003% NP-40, 0.3 mM DTT. The annealing reaction was heated for 5 min at 75 °C and allowed to cool slowly to room temperature. Fluorescence measurements were performed utilizing an Instruments S. A., Inc., fluorolog-3 spectrophotometer. Excitation was at 310 nm, and fluorescence emission was scanned from 335 to 430 nm. Slit widths of 5.0 nm were used for excitation and emission for all experiments. Spectra were obtained for solutions containing 0.8 μM RNA with or without 1.5 μM ADAR2 in 36 mM Tris-HCl, pH 7.5, 7% glycerol, 142 mM KCl, 3.6 mM EDTA, 0.007% NP-40, 0.7 mM DTT at room temperature. The background fluorescence of the enzyme was subtracted from the spectrum of the complex.

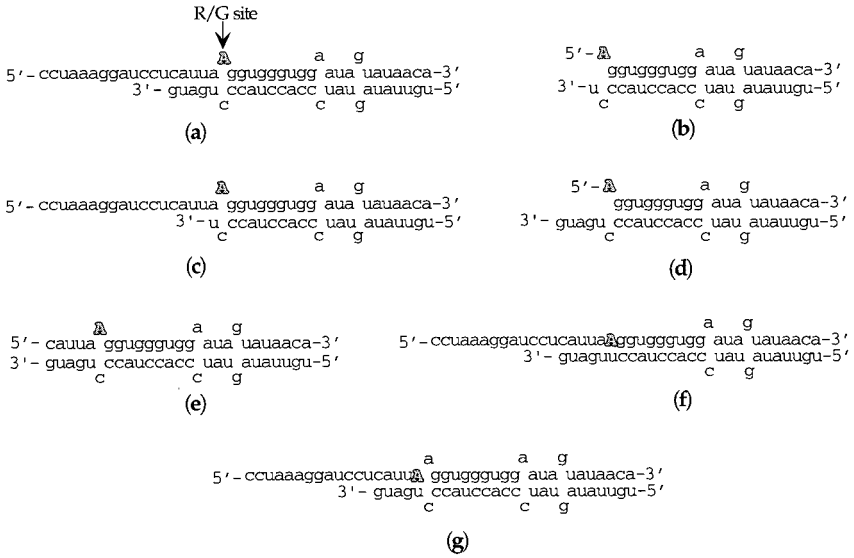

FIGURE 2: Duplex RNA substrates of ADAR2 used in this study. The capitalized, outlined adenosine in each substrate is site-specifically-labeled at its 5′-phosphate with ^{32}P (See Materials and Methods for preparation). R/G site refers to the position analogous to the adenosine located at the arginine to glycine editing site found in the GluR-B subunit pre-mRNA.

RESULTS

Preparation of Duplex Substrates for Analysis of Deamination Kinetics. For these studies, we prepared RNA duplexes of the sequence found near the R/G editing site of the GluR-B pre-mRNA that were site-specifically ^{32}P-labeled such that deamination could be monitored at a specific adenosine (*17*). For duplexes with adenosine at the 5′ end, an oligonucleotide was simply end-labeled using T4 kinase and [γ-^{32}P]ATP. For duplexes with internally labeled adenosines, the substrates were assembled using a splinted ligation strategy and two RNA oligonucleotides, one having a 5′-^{32}P-labeled adenosine (*15*). Once the labeled single-stranded oligonucleotides were obtained, the necessary duplexes were formed by hybridization to the complementary strands. The seven duplex substrates used in this study are shown in Figure 2. Substrates (**a**)−(**f**) differ in structure at the R/G editing site and to the 5′ side of the R/G editing site. Each has the R/G site adenosine specifically labeled. Substrate (**g**) is the same sequence as (**a**) but with the adenosine immediately adjacent to the R/G site labeled.

For substrate (**e**), with only five base pairs 5′ to the edited adenosine, a standard splint ligation was not successful. This is likely due to the low stability of the 5 bp duplex formed on the splint. In this case, an 18-mer chimeric DNA/RNA oligonucleotide with 13 nt of DNA and 5 nt of RNA was used during the ligation (see Materials and Methods). After the ligation, the deoxyribonucleotides were removed by DNase I digestion, and the 27-mer RNA oligonucleotide internally ^{32}P labeled at the R/G editing site was purified from the DNase I reaction by PAGE.

Single Turnover and Steady-State Kinetics of an RNA Editing Reaction. The rate of deamination at the adenosine corresponding to the R/G site was measured for substrate (**a**) under single turnover conditions (100 nM ADAR2, 25 nM substrate) (Figure 3A,B). This substrate has duplex secondary structure on both sides of the editing site and a 13 nt 5′ overhang of sequence found in the GluR-B pre-mRNA. The 5′ overhang is a consequence of the oligonucleotides chosen for the splint ligation necessary to site specifically label this substrate and does not appreciably contribute to the single turnover rate (see below). Progress of the reaction was followed using the thin-layer chromatography assay previously described that allows for the separation and quantification of ^{32}P-labeled AMP and IMP arising from the nuclease digestion of substrate and product (*16*). Under these conditions, substrate (**a**) was converted to product with an end point of ~85% and with a first-order rate constant $k_{deam} = 1.2 \pm 0.1$ min^{-1}. This rate is >15-fold higher than that measured for synthetic substrates bearing the editing site at the 5′ end of a duplex (see below) (*18*).

Steady-state rate analyses are problematic for RNA substrates that are processed slowly by ADAR2. Due to the slow rate of a single turnover, the time required to reach the steady state makes enzyme denaturation a concern. Steady-state rate experiments seemed more feasible with an RNA substrate with a single turnover rate constant of >1 min^{-1} for deamination at a specific adenosine. Indeed, when (**a**) was analyzed under conditions of a large excess of substrate (800 nM substrate RNA, 30 nM ADAR2), product formation was linear with time up to ~90 nM (three turnovers) (Figure 3C). The *y*-intercept of the linear fit was zero with no apparent burst of product corresponding to the first turnover. The slope of the line fit to these data is 13 ± 1.5 nM·min^{-1} for a $k_{ss} = 0.43 \pm 0.05$ min^{-1}. A 2-fold change in substrate concentration did not affect the measured rate (data not shown). Also, gel mobility shift experiments suggest that this concentration of substrate is significantly higher than the dissociation constant (see below).

Comparison of ADAR2 Substrates Using Single Turnover Kinetics. To define the origin of the increased rate of deamination seen with (**a**) compared to duplexes studied previously (*18*), we compared the rate of deamination of the R/G site adenosine in substrates (**b**)−(**e**) under single turnover conditions (Figure 4) (Table 1). Under these conditions, substrate (**b**), with the reactive adenosine at the 5′ end of the duplex, was deaminated by ADAR2 with a $k_{deam} = 0.038 \pm 0.005$ min^{-1}. Both substrate (**c**), with only the top strand extension, and substrate (**d**), with only the

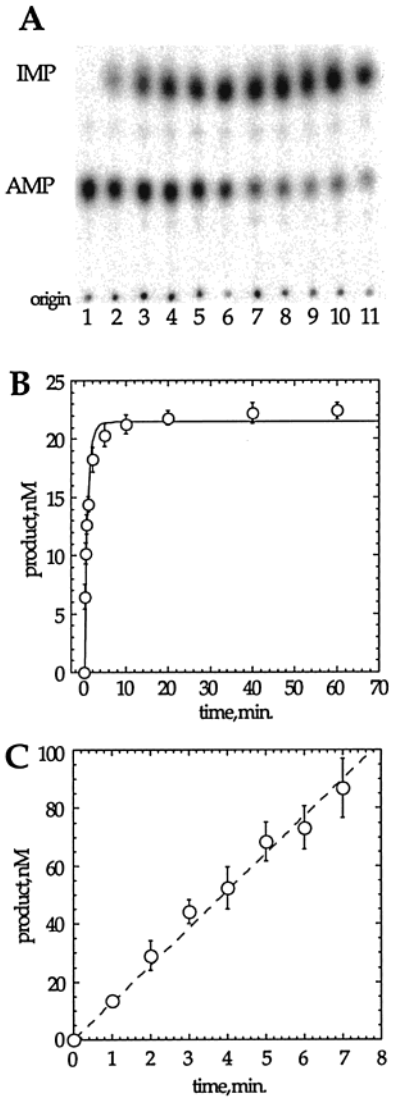

FIGURE 3: (A) Single turnover kinetics of the reaction of ADAR2 with substrate (**a**). Storage phosphor autoradiogram of TLC plate used to separate deamination products arising from reaction of 100 nM ADAR2 with 25 nM substrate (**a**). Lanes 1−11: Reaction times of 0, 0.25, 0.5, 0.75, 1, 2, 5, 10, 20, 40, and 60 min, respectively. (B) Plot of product formation as a function of time for the single turnover reaction of ADAR2 and substrate (**a**). The data were fit to the equation $[P]_t = \alpha[1 - e^{(-k_{deam}t)}]$ using the least-squares method of KaleidaGraph. Data points reported are the average ± standard deviation for three independent experiments. (C) Steady-state rate analysis of the reaction of ADAR2 with substrate (**a**). Plot of product formation as a function of time for the reaction of 30 nM ADAR2 with 800 nM substrate (**a**). Data points reported are the average ± standard deviation for three independent experiments.

bottom strand extension, are deaminated >15-fold slower than (**a**). Therefore, the 32-fold higher rate observed with (**a**) compared to (**b**) is largely a result of the extension of both strands. It does appear that extension of the top strand has a greater effect on the reaction than extension of the bottom strand; substrate (**c**) is processed more efficiently (higher rate and yield) than is substrate (**d**). The 5′ single-stranded overhang of substrate (**a**) does not significantly contribute to the rate of deamination as substrate (**e**), lacking any single-stranded overhangs, reacts at essentially the same rate as (**a**).

Substrates (**a**) and (**e**) have duplex on both sides of the editing site and have the reactive adenosine in an A·C mismatch. To determine the extent to which this destabilizing pairing contributes to the reactivity, we prepared duplex (**f**), similar in structure to (**a**) but with an A·U pair at the editing site, and measured the deamination rate at this site under single turnover conditions. This substrate is processed at a rate only 4-fold lower than (**a**), suggesting that the base pairing partner for the adenosine is not a critical determinant for the relative rates of deamination at different sites (Figure 4) (Table 1).

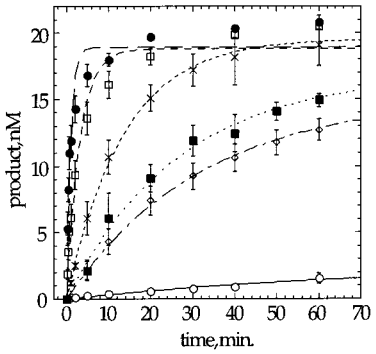

FIGURE 4: Single turnover kinetics of the reaction of ADAR2 with substrates (**b**)−(**g**). Plot of product formation as a function of time for the reaction of 100 nM ADAR2 with 25 nM substrate. (■) = substrate (**b**), (×) = substrate (**c**), (◇) = substrate (**d**), (●) = substrate (**e**), (□) = substrate (**f**), (○) = substrate (**g**). The data were fit to the equation $[P]_t = \alpha[1 - e^{(-k_{deam}t)}]$ using the least-squares method of KaleidaGraph. Data points reported are the average ± standard deviation for three independent experiments.

Table 1: Single Turnover Kinetic Parameters for the Adenosine Deamination of Duplex Substrates by ADAR2[a]

substrate	α, nM[b]	k_{deam}, min^{-1}	k_{rel}[c]
(**a**)	21.5 ± 0.7	1.2 ± 0.1	1.0
(**b**)	16.9 ± 0.4	0.038 ± 0.005	32
(**c**)	19 ± 1	0.07 ± 0.01	17
(**d**)	15.2 ± 0.7	0.031 ± 0.004	39
(**e**)	18.9 ± 0.1	1.0 ± 0.2	1.2
(**f**)	18.8 ± 0.2	0.32 ± 0.08	3.7
(**g**)	2.7 ± 0.1	0.013 ± 0.004	92

[a] Single turnover deamination reactions were carried out with 100 nM ADAR2, 25 nM RNA substrate in 15 mM Tris-HCl, pH 7.1, 3% glycerol, 0.5 mM DTT, 60 mM KCl, 1.5 mM EDTA, 0.003% NP-40, 160 units/mL RNasin, and 1.0 μg/mL yeast $tRNA^{Phe}$. [b] Data were fit to the equation: $[P]_t = \alpha[1 - e^{(-k_{deam}t)}]$. [c] k_{rel} is equal to the k_{deam} determined for substrate (**a**)/k_{deam} for each substrate.

Substrate (**g**), which has the same structure as (**a**), but with the adenosine immediately adjacent to the R/G site labeled, was designed to determine if the selectivity observed for ADAR2 editing on longer RNAs is retained in our synthetic models (*6*). This adenosine is deaminated to a low level (~10%) and at a rate >90-fold slower than the R/G site (Figure 4) (Table 1). Furthermore, by ribonuclease sequencing the products of a 1 h ADAR2 reaction with substrate (**e**), we detect only the R/G site adenosine converted to inosine (data not shown). Therefore, this relatively small RNA structure retains elements that lead to selective deamination at the editing site. Furthermore, this result illustrates the significant effect of the structural context of a given adenosine in determining the rate of ADAR2-catalyzed deamination at that site.

Binding of ADAR2 Substrates Measured by a Gel Mobility Shift Assay. The differences in single turnover rate constants determined for substrates that have duplex on both sides of

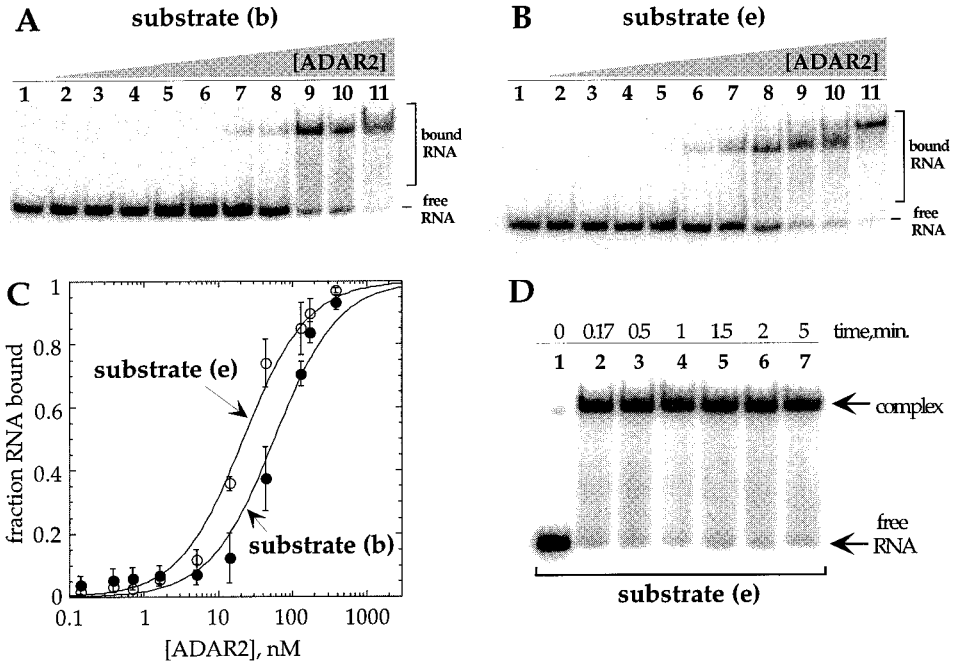

FIGURE 5: Quantitative gel mobility shift analysis of the binding of ADAR2 to duplex RNA substrates (**b**) and (**e**). (A) Storage phosphor autoradiogram of gel used to separate bound from free substrate (**b**). Lanes 1−11: 0, 0.1, 0.4, 0.7, 1.6, 5.0, 14, 43, 129, 172, and 387 nM ADAR2 added. (B) Storage phosphor autoradiogram of gel used to separate bound from free substrate (**e**). Lanes 1−11: 0, 0.1, 0.4, 0.7, 1.6, 5.0, 14, 43, 129, 172, and 387 nM ADAR2 added. (C) Plots of the fraction of RNA bound as a function of ADAR2 concentration; (●) = substrate (**b**), (○) = substrate (**e**). The data were fit to the equation: fraction bound = [ADAR2]/([ADAR2] + K_d^{app}) using the least-squares method of KaleidaGraph. Data points reported are the average ± standard deviation for three independent experiments. (D) Time course of the binding of ADAR2 to substrate (**e**) under the conditions of the single turnover kinetic analysis (100 nM ADAR2, 25 nM substrate). Samples were incubated under the reaction conditions for the times indicated and then loaded onto a running 6% nondenaturing polyacrylamide gel. Lane 1: no ADAR2. Lanes 2−7: 0.17, 0.5, 1, 1.5, 2, 5 min incubation after addition of ADAR2.

the editing site versus those that do not prompted us to determine the effect this feature had on the substrate binding affinity for ADAR2. For this purpose, substrates (**b**) and (**e**) were analyzed using a quantitative gel mobility shift assay (Figure 5). These duplexes are representative good (**e**) and poor (**b**) substrates. For each substrate, complexation was observed upon addition of increasing concentrations of protein. ADAR2 bound substrate (**e**) with an apparent dissociation constant (K_d^{app}) of 22 ± 4 nM and substrate (**b**) with a K_d^{app} = 52 ± 3 nM. This relatively minor difference in binding affinity indicates that the large differences in rate observed likely arise from differences in steps after complexation.

The rate of formation of the complex between ADAR2 and substrate (**e**) under single turnover conditions (25 nM RNA, 100 nM ADAR2) was too fast to measure using this gel mobility shift assay; the binding reaction was complete as soon as the mixture could be loaded onto the electrophoresis gel (Figure 5D). The length of time necessary for the complexes to move into the gel was estimated to be no more than 90 s, and the binding was >95% complete at this time point. Therefore, a lower limit of ~2 min^{-1} can be placed on the binding rate constant. Although this value is similar in magnitude to the measured deamination rate constant for this substrate (1 min^{-1}), it is unlikely that binding is limiting the single turnover rate as increasing the substrate concentration does not significantly increase the measured deamination rate (data not shown).

ADAR2-Induced Changes in the Fluorescence of an RNA Substrate Containing 2-Aminopurine at an Editing Site. 2-Aminopurine (2-AP) is a fluorescent nucleic acid base analogue whose quantum yield and emission λ_{max} are sensitive to its electronic environment (*19*). When free in solution or present in single-stranded oligonucleotides, 2-AP is highly fluorescent. However, when present in a base paired duplex, the 2-AP fluorescence is quenched. Furthermore, the 2-AP emission maximum is sensitive to the hydrophobicity of its environment. Together, these properties have made 2-AP a useful probe of the base flipping step in the reactions of nucleic acid-modifying enzymes (*20*−*23*). To determine if monitoring changes in 2-AP fluorescence could be used to study ADAR2-induced structural changes in its RNA substrate, we prepared a variant of substrate (**e**) that had the adenosine at the R/G site replaced with 2-AP (Figure 6). As expected, the single-stranded 2-AP-containing oligonucleotide was highly fluorescent with an emission maximum at 372 nm (λ^{ex} = 310 nm). Duplex formation decreased the emission intensity 4-fold with little effect on the wavelength of the emission maximum. When 1.5 μM ADAR2 was added to 0.8 μM of this duplex, the emission intensity increased by 3.3-fold and the maximum shifted to 359 nm (Figure 6). These changes in fluorescence occurred rapidly with little additional change in the spectrum after 30 s and up to 20 min.

DISCUSSION

Effect of Structure 5′ to the Editing Site. Previously, we showed that RNA duplexes prepared by chemical synthesis would support the adenosine deamination reaction catalyzed by ADAR2 (*18*). These substrates were similar in length and sequence to a hairpin stem found naturally in the GluR-B pre-mRNA (*5*). An important difference between our model

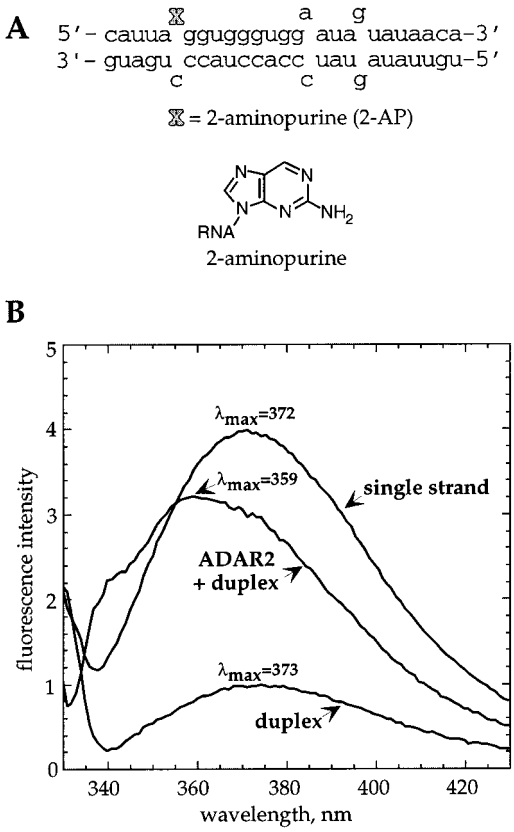

FIGURE 6: (A) Fluorescent ADAR2 substrate analogue with 2-aminopurine (2-AP) at the editing site. (B) Plot of fluorescence intensity ($\lambda^{ex} = 310$ nm) as a function of wavelength scanned for 0.8 μM 2-AP-containing single strand, 0.8 μM duplex, and 0.8 μM duplex in the presence of 1.5 μM ADAR2. Fluorescence intensity is plotted in arbitrary units. Each spectrum is an average of three independent measurements.

duplexes and the natural substrate was the placement of the reactive adenosine at the 5′ end of the duplex structure, omitting the five base pairs predicted to be found in the natural hairpin stem 5′ to the R/G editing site (*5*). Prior to our work, others had shown that these base pairs were not a requirement for R/G site editing by ADAR2 (*17*). However, these analyses were carried out by determining the percent editing after long incubation times (4 h). Significant differences in reaction rates would not have been detected. In addition, the relatively slow reaction rates we observed with truncated substrates (*18*) led us to determine to what extent structure 5′ to the editing site could contribute to the ADAR2 reaction at the R/G site. Naturally occurring ADAR substrates identified to date also have the reactive adenosines embedded in duplex secondary structure (*3*−*5*, *24*). Therefore, a conformational change in the RNA that flips the adenosine out of the helix core is likely an important step in the reaction mechanism. We sought model substrates for kinetic and biophysical studies that retained this feature. For these experiments, we assembled RNA substrates of varying structure and sequence that either did or did not have the reactive adenosine embedded in a duplex (Figure 2). Substrates (**a**) and (**e**), each with duplex on both sides of the deamination site, were the best substrates identified (Table 1). The increased rate relative to the substrates without base pairing 5′ to the editing site appears to arise from transition state stabilization and not from substrate binding as the binding constants for substrates (**b**) and (**e**) differed only slightly (2.4-fold) (Figure 5). Duplex structure to the 3′ side of the reactive adenosine had been previously shown to be essential for reaction at the R/G site, likely as the binding site for the ADAR's dsRBMs (*5*, *18*, *25*). The effect of base pairing 5′ to the editing site observed here suggests the existence of stabilizing contacts made by ADAR2 to the double helix on both sides of the editing site. This result is consistent with recently reported footprinting experiments, which indicate that ADAR2 protects base pairs in the RNA duplex flanking the R/G editing site (*26*). Several nucleic acid modifying enzymes that extrude the reactive nucleotide from a double helix have been studied by X-ray crystallography in complex with their nucleic acid ligands (*27*−*29*). Contacts to the duplex both upstream and downstream of the target nucleotide are a common feature of these structures. For instance, *Hha*I DNA cytidine methyltransferase, which flips a cytidine out of the DNA helix for methylation at carbon 5, makes contacts to both strands of the duplex across the 8 bp that surround the reactive cytidine (*27*). The DNA repair enzyme endonuclease IV contacts both strands of duplex DNA over the 6 bp that surround an abasic site, where it flips out both the abasic nucleotide and the nucleotide across the duplex, cleaving the strand containing the abasic site (*28*). Interestingly, uracil DNA glycosylase, which cleaves uracil from DNA duplexes, makes extensive contacts to the uracil-containing strand and only a single contact to the complementary strand (*29*). Comparing substrates (**c**) and (**d**) in this work suggests that contacts to the adenosine-containing strand may be more important in the ADAR2 reaction at the R/G site.

In our initial comparison of substrates (**a**)−(**d**), we could not rule out the 5′ single-stranded overhang as contributing to the enhanced rate of (**a**). This overhang is a result of the oligonucleotides chosen for efficient splint ligation and is composed of GluR-B pre-mRNA sequence. Therefore, it was possible that this sequence favorably interacted with ADAR2. By carrying out the splint ligation with a DNA/RNA chimera, we could prepare a substrate that had no 5′ single-stranded overhang and directly measure its effect on the reaction. Since the rate of deamination for this substrate was essentially the same as for substrate (**a**), nucleotides in the 5′ overhang do not contribute to R/G site deamination.

Effect of Sequence on the Editing Reaction. Several groups have used various techniques to measure percent editing at a single time point for a specific adenosine and addressed the effect of sequence changes on an ADAR reaction (*4*, *12*, *17*, *25*, *30*). However, prior to this work, rate constants for the deamination at a single adenosine in different sequence environments had not been reported. Measuring relative rates for deamination at specific adenosines and defining the factors that affect the rate-determining step will be critical to understanding the reaction mechanism and the energetic basis for selectivity (*31*). Comparing the reaction of substrates (**a**) and (**g**), it is clear that there is a significant sequence context effect on the ADAR2 reaction rate. These two substrates differ only in which adenosine is labeled with ^{32}P for analysis of the deamination reaction. There is a >90-fold preference for reaction at the R/G site over the adjacent adenosine. This is a conservative estimate of the relative rates because the adjacent adenosine is converted to only ~10% product compared to ~85% for the R/G site over the course of the reaction. These two adenosines differ in their flanking

sequence environment, in their pairing interactions, and in their locations on the duplex relative to the ends and base mismatches. However, the identity of the pairing partner has a relatively minor effect as substrate (**f**), which has the R/G site adenosine in an A·U base pair, reacts only 4-fold slower than substrate (**a**). The proximity of an adenosine to duplex deformations has been shown to be an important factor in controlling the selectivity of ADAR1 (*32*). Thus, the low reactivity of the adenosine adjacent to the R/G site could arise from its juxtaposition to the A·C mismatch at the R/G site. However, we found that converting this A·C mismatch to an A·U base pair did not increase the efficiency of the ADAR2 reaction at the adjacent adenosine (data not shown). Further experiments will be necessary to determine the basis for selectivity of ADAR2 for the R/G site versus the adjacent adenosine. It is possible that ADAR2 makes contacts to the RNA structure, either 5′ or 3′ to the editing site, that are sequence dependent.

Analysis of Turnover at the R/G Site. A steady-state rate measurement was carried out with substrate (**a**) to assess ADAR2's ability to turn over at the R/G site. Similar experiments with substrates bearing a 5′ editing site were complicated by extremely slow reactions at high substrate concentrations, suggestive of substrate inhibition. The rate of enzyme denaturation competed with the rate of deamination during the long incubation times required to reach the steady state with these substrates. However, at 800 nM substrate (**a**) and 30 nM ADAR2, product formation was linear with time for 7 min and through three turnovers. The lack of an initial burst of product suggests that the rate constant for the rate-limiting step of the first turnover is similar in magnitude to that of the rate-limiting step for subsequent turnovers. Therefore, these rate-limiting steps could be the same. This interpretation is consistent with the comparison of the single turnover rate constant for this substrate (1.2 min^{-1}, determined at 100 nM ADAR2, 25 nM substrate) being within 3-fold of the measured steady-state rate constant (0.43 min^{-1}, determined at 30 nM ADAR2, 800 nM substrate). Possibilities for the rate-limiting step include conformational changes in the RNA·protein complex, as well as chemical steps in the conversion of adenosine to inosine in the deamination active site.

Evidence for an ADAR2-Induced Conformational Change in the RNA Substrate. The necessary trajectory for nucleophilic attack at C6 of adenosine makes it likely that ADAR2 flips its target nucleotide out of the RNA helix core. Indeed, sequence analysis of the family of ADAR-like enzymes indicated that conserved sequence motifs exist in this family that are remarkably similar to conserved motifs in the family of cytidine and adenosine DNA methyltransferases, enzymes that are known to extrude the reactive nucleotide (*10*). Included in the commonly conserved sequences are amino acids that have been proposed to create a binding pocket for the flipped-out adenosine in the reaction of N6 adenosine DNA methyltransferases (*33*). However, no experimental evidence for a base flipping conformational change during the ADAR-catalyzed editing reaction has been reported.

The base flipping step in two different N6 adenosine DNA methyltransferases (M.*Taq*I and M.*Eco*RI) has been studied by monitoring enzyme-induced changes in the fluorescence of 2-AP-modified substrates (*21*, *22*). When the 2-AP is located at the site of the adenine to be methylated, M.*Eco*RI induces an increase in fluorescence intensity of the DNA duplex 14-fold with a 10 nm blue shift in the emission maximum to $\lambda_{max} = 359$ nm (*22*). M.*Taq*I causes a 13-fold increase in intensity with an emission $\lambda_{max} = 357$ nm for the protein·DNA complex (*21*). The 3.3-fold increase in 2-AP fluorescence intensity with a blue-shifted maximum of 359 nm reported here for an ADAR2 substrate modified at the editing site is consistent with ADAR2 flipping out the reactive adenosine into a binding pocket similar in nature to that of the adenosine methyltransferases. The lower enhancement of 2-AP fluorescence observed with ADAR2 compared to that of the methyltransferases could be due to several factors. This may be a consequence of the 2-AP·C mismatch at the editing site as base mismatches have been shown to be less effective at quenching the 2-AP fluorescence than base pairs (*21*). This would have the effect of increasing the duplex fluorescence relative to the duplexes used to study the methyltransferases. Alternatively, the 2-amino modification of the purine may adversely affect the interaction between the flipped out base and its binding pocket. In support of this hypothesis, we find that 2,6-diaminopurine at the R/G editing site is a poor substrate for ADAR2 (Easterwood, L. E., Veliz, E. A., Beal, P. A., manuscript in preparation). Nevertheless, the substantial increase in the fluorescence of the 2-AP-containing duplex and the fact that the ADAR2·2-AP-RNA complex has an emission λ_{max} (359 nm) similar to that of the M.*Eco*RI·2-AP-DNA complex (359 nm) and M.*Taq*I·2-AP-DNA complex (357 nm) support a base flipping mechanism for ADAR2. Interestingly, the fact that no changes in the fluorescence spectrum were observed after 30 s suggests that base flipping is rapid relative to deamination for this substrate. Stopped-flow fluorescence measurements should allow for an accurate determination of the rate of flipping at the R/G site and other sites in an ADAR substrate (*23*). A comparison of these rates may provide further insight into the basis for ADAR selectivity.

Impact on Future Studies with ADAR2. Through the work reported here, we have identified synthetically accessible ADAR2 substrates with the reactive adenosine embedded in duplex secondary structure for which both single turnover and steady-state rate analyses for deamination at a specific adenosine are practical. Variants of this substrate bearing sequence changes and/or diagnostic nucleotide analogues, such as 2-AP, will be useful in further defining the ADAR2 mechanism. In addition, duplexes similar in structure to substrate (**e**) containing mimics of the proposed deamination transition state located at the R/G site will be useful reagents for future biophysical studies of the ADAR2·RNA complex.

ACKNOWLEDGMENT

We thank Prof. Brenda Bass, Herbert L. Ley III, and Arunth T. Lingam in the Department of Biochemistry, University of Utah, for the *S. cerevisiae* overexpression system for human ADAR2, advice, helpful discussion, and technical assistance.

REFERENCES

1. Grosjean, H., and Benne, R. (1998) *Modification and Editing of RNA*, ASM Press, Washington, DC.
2. Patton, D. E., Silva, T., and Bezanilla, F. (1997) *Neuron 19*, 711−722.

3. Burns, C. M., Chu, H., Rueter, S. M., Hutchinson, L. K., Canton, H., Sanders-Bush, E., and Emeson, R. B. (1997) *Nature 387*, 303−308.
4. Higuchi, M., Single, F. N., Kohler, M., Sommer, B., Sprengel, R., and Seeburg, P. H. (1993) *Cell 75*, 1361−1370.
5. Lomeli, H., Mosbacher, J., Melcher, T., Hoger, T., Geiger, J. R. P., Kuner, T., Monyer, H., Higuchi, M., Bach, A., and Seeburg, P. H. (1994) *Science 266*, 1709−1713.
6. O'Connell, M. A., Gerber, A., and Keller, W. (1997) *J. Biol. Chem. 272*, 473−478.
7. Melcher, T., Maas, S., Herb, A., Sprengel, R., Seeburg, P. H., and Higuchi, M. (1996) *Nature 379*, 460−464.
8. Fierro-Monti, I., and Mathews, M. B. (2000) *Trends Biochem. Sci. 25*, 241−246.
9. Lai, F., Drakas, R., and Nishikura, K. (1995) *J. Biol. Chem. 270*, 17098−17105.
10. Hough, R. F., and Bass, B. L. (1997) *RNA 3*, 356−370.
11. Carter, C. W. (1995) *Biochemie 77*, 92−98.
12. Gerber, A., Grosjean, H., Melcher, T., and Keller, W. (1998) *EMBO J. 17*, 4780−4789.
13. Polson, A. G., Crain, P. F., Pomerantz, S. C., McCloskey, J. A., and Bass, B. L. (1991) *Biochemistry 30*, 11507−11514.
14. Cantor, C. R., and Tinoco, I. (1965) *J. Mol. Biol. 13*, 65−77.
15. Moore, M. J., and Sharp, P. A. (1992) *Science 256*, 992−997.
16. Bass, B. L., and Weintraub, H. (1988) *Cell 55*, 1089−1098.
17. Yang, J.-H., Sklar, P., Axel, R., and Maniatis, T. (1997) *Proc. Natl. Acad. Sci. U.S.A. 94*, 4354−4359.
18. Yi-Brunozzi, H.-Y., Easterwood, L. M., Kamilar, G. M., and Beal, P. A. (1999) *Nucleic Acids Res. 27*, 2912−2917.
19. Ward, D. C., Reich, E., and Stryer, L. (1969) *J. Biol. Chem. 244*, 1228−1237.
20. Stivers, J. T., Pankiewicz, K. W., and Watanabe, K. A. (1999) *Biochemistry 38*, 952−963.
21. Holz, B., Klimasauskas, S., Serva, S., and Weinhold, E. (1998) *Nucleic Acids Res. 26*, 1076−1083.
22. Allan, B. W., and Reich, N. O. (1996) *Biochemistry 35*, 14757−14762.
23. Allan, B. W., Reich, N. O., and Beechem, J. M. (1999) *Biochemistry 38*, 5308−5314.
24. Polson, A. G., Bass, B. L., and Casey, J. L. (1996) *Nature 380*, 454−456.
25. Aruscavage, P. J., and Bass, B. L. (2000) *RNA 6*, 257−269.
26. Ohman, M., Kallman, A. M., and Bass, B. L. (2000) *RNA 6*, 687−697.
27. Klimasauskas, S., Kumar, S., Roberts, R. J., and Cheng, X. (1994) *Cell 76*, 357−369.
28. Hosfield, D. J., Guan, Y., Haas, B. J., Cunningham, R. P., and Tainer, J. A. (1999) *Cell 98*, 397−408.
29. Slupphaug, G., Mol, C. D., Kavli, B., Arvai, A. S., Krokan, H. E., and Tainer, J. A. (1996) *Nature 384*, 87−92.
30. Maas, S., Melcher, T., Herb, A., Seeburg, P. H., Keller, W., Krause, S., Higuchi, M., and O'Connell, M. A. (1996) *J. Biol. Chem. 271*, 12221−12226.
31. Lesser, D. R., Kurpiewski, M. R., and Jen-Jacobson, L. (1990) *Science 250*, 776−786.
32. Lehmann, K. A., and Bass, B. L. (1999) *J. Mol. Biol. 291*, 1−13.
33. Malone, T., Blumenthal, R. M., and Cheng, X. (1995) *J. Mol. Biol. 253*, 618−632.

BI0011577